



## Synthesis of Linde Type A zeolite from Darazo kaolin found in Bauchi State, Nigeria

Ikenna Ekpe<sup>1,\*</sup>, Henry Mgbemere<sup>2</sup>, Ganiyu Lawal<sup>2</sup>, Henry Ovri<sup>3</sup>, Anna L. Sargent<sup>4</sup>

<sup>1</sup>Department of Mechanical Engineering, Covenant University, Ogun, Nigeria

<sup>2</sup>Department of Metallurgical and Materials Engineering, University of Lagos, Lagos, Nigeria

<sup>3</sup>Department of Experimental Mechanics, Institute of Materials Research, Geesthacht, Germany

<sup>4</sup>Institute of Photoelectrochemistry, Geesthacht, Germany

\*Corresponding author: ikenna.ekpe@covenantuniversity.edu.ng

Received 20 May 2022

Revised 26 July 2022

Accepted 4 August 2022

### Abstract

The hydrothermal method of zeolite synthesis was used to obtain the Linde Type A (LTA) zeolites from kaolin found in Darazo. Characterization confirms the presence of alumina and silica which are the precursor materials for zeolite synthesis. The Fourier Transform Infrared Spectroscopy (FTIR) and X-ray diffraction (XRD) analyses indicate the presence of characteristic zeolite peaks while the scanning electron microscope (SEM) shows clearly defined cubic zeolite-A crystals. In addition, a water adsorption test on the synthesized LTA zeolites showed good water adsorption capacities of 27.96 and 28.01% for samples calcined at 700 and 900°C respectively. Such results enable these materials to be good candidates for water adsorption applications. These experiments show that LTA zeolites can successfully be synthesized from kaolin found in the Darazo area using the hydrothermal process of zeolite synthesis with similar results obtained for both LTA zeolites produced from Darazo kaolin calcined at 700 and 900°C. A comparison of the different calcination temperatures for the LTA zeolites shows that the materials calcined at 900°C give better adsorption properties.

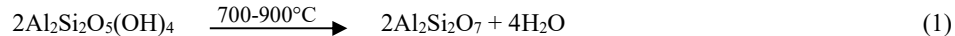
**Keywords:** Darazo, Hydrothermal method, Kaolin, Metakaolin, Zeolite

### 1. Introduction

Zeolites are microporous crystals made from aluminosilicate materials with significant scientific, and industrial applications such as ion exchangers (as used in the treatment of liquid waste, radioactive waste storage, and the detergent industry), separation media (for water purification, drying, and molecular sieve) and petroleum refining [1-3]. The capacity of zeolites to play a multi-functional role is due to their inherent wide-ranging properties including good hydrophilicity, uniform pore size/shape, high catalytic activity, and highly mobile cations [4]. Synthetic zeolites are used as adsorbents for gases and vapors in industrial processes as well as catalysts especially used in the petroleum industry [5]. They are also used in the drying of liquids and gases in low humidity conditions and when compared to conventional adsorbents, have higher adsorption capacity for gases and liquids. They also show higher absorption capacities for polar compounds such as water, NH<sub>3</sub>, CO<sub>2</sub>, SO<sub>2</sub>, and H<sub>2</sub>S even at temperatures as low as 273 K. Traditionally, synthetic zeolites are produced using the hydrothermal method with SiO<sub>2</sub> and Al<sub>2</sub>O<sub>3</sub> serving as the precursor materials [6]. Additionally, the use of kaolin in the synthesis of zeolites primarily to obtain silica and alumina has been investigated with positive results [5,7,8]. Kaolin is inexpensive, readily available, and a relatively abundant raw material [9]. The cost comparison between the use of kaolin as precursor materials for zeolite synthesis has been studied [10]. and the results show that kaolin has a comparative cost reduction of about 15% over the use of commercial chemicals. This research work aims to prepare linde type A (LTA) zeolites using kaolin found in the area of Darazo, Nigeria, and to characterize it with respect to its adsorption, thermal, and other functional properties.

## 2. Materials and methods

In this study, the materials used include kaolinite obtained from the Darazo region, in Bauchi State, Nigeria, NaOH (97% purity), together with deionized water. The following procedure was used to prepare the LTA zeolites: the kaolin, as supplied from the source, was purified from physically bonded impurities by crushing, grinding, and soaking in deionized water for 24 h after which the water was removed through decanting. A 200 (i.e., 75  $\mu\text{m}$  aperture opening) mesh size Tyler sieve was used to sieve the resulting residue, and then the larger particles were allowed to settle. At regular intervals, the topwater was decanted and the residue placed in a clean sac and pressed under a heavy load leading to the formation of cake-like kaolin. The cake was dried for 3 days and a ball mill operating at a speed of 60 rpm for 6 h was used to pulverize the kaolinite. The resulting ball-milled kaolinite was calcined in a muffle furnace for 2 h at two different temperatures of 700 and 900°C. This process is believed to convert the unreactive kaolin to a reactive but less stable metakaolin as represented in Reaction 1.



NaOH, deionized water, and the resulting metakaolinite were mixed to form a solution in the ratio of 0.6: 0.8: 12 by weight. The solution was allowed to stand for 24 h while being stirred intermittently. To obtain the required zeolites, a crystallization process was used by placing the solution in an oven for 6 h at 100°C. The procedure is described as seen in Reaction 2 below.



After crystallization, the excess sodium hydroxide was removed through the washing of the product. The solvent was decanted and placed into an oven for 6 h at 110°C to dry the residual LTA zeolite crystals.

### 2.1 Sample characterization

X-ray Fluorescence (XRF) was performed using the Horiba XGT 5000 model which employed the energy-dispersive method (EDXRF) to analyze the components of both the Darazo kaolinite and the synthesized LTA zeolite samples. The samples were pressed into 6 mm diameter pellets. Wax was used as the binder material with a wax to sample ratio of 3:11 by weight.

A Netzsch STA 409 C analyzer was used to perform the differential thermal analysis (DTA)/thermogravimetric (TG) analysis in a 50 mL/min argon flow with a heating rate of 5°C /min from 20 to 800°C. The X-ray diffraction (XRD) measurements were carried out using synchrotron diffraction. A wavelength ( $\lambda$ ) of 0.20716 Å and photon energy of 60 KeV were used to carry out the measurements. Data collection was done at radially integrated 5° steps with the aid of a Perkins Elmer 2D detector.

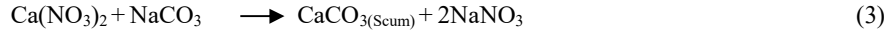
A Shimadzu IR Affinity-1S was used for the Fourier Transform Infrared Spectroscopy (FTIR) spectroscopy where the samples were mixed with KBr and pressed into pellets (with a diameter of 10 mm) and then placed under a lamp in a pre-heated die. The pellets were out-gassed at 120°C for 1 h before obtaining the spectra in transmission mode.

The morphologies of the kaolin and zeolite were studied using an ASPEX 3020 scanning electron microscope (SEM). About 1.0 mg of the sample was treated with acetone to ensure particle dispersion. Once the solvent had evaporated, samples were then placed in a vacuum chamber and sputtered with gold for improved electrical contact during SEM operation. The images were acquired using the secondary electron imaging mode at a magnification of 8000 and a working distance of 10.1 mm.

A Micromeritics ASAP 2020 porosity analyzer was used to analyze the nitrogen adsorption and surface area of the zeolite. The samples were degassed for 40 h under vacuum at 80°C and for 8 h, then further degassed at 350°C prior to the nitrogen sorption measurements.

The zeolite water adsorption capacities were determined by measuring the weight of the adsorbate absorbed. A milli-equivalent or percentage of the adsorbate was used to represent the result. A simply designed laboratory apparatus was used to test the adsorption capacity of the LTA zeolites where water vapor saturated with air was passed over a sample with a known weight. Under these conditions, the LTA zeolites absorbed water, and the resultant increase in weight of the zeolite was taken after 24 h.

The ion exchange capacity tests were carried out using  $\text{Na}_2\text{CO}_3$ ,  $\text{CaO}$ , and deionized water. For the control sample, 10 ml of deionized water was measured into a 250 mL beaker containing 0.2 g of  $\text{Na}_2\text{CO}_3$  and  $\text{Ca}(\text{NO}_3)_2$  and stirred vigorously.  $\text{Ca}^{2+}$  is higher than  $\text{Na}^+$  in the electrochemical series and will displace  $\text{Na}^+$  in any chemical reaction with the result being the formation of a  $\text{CaCO}_3$  precipitate with a pH value of 10.98, as in shown in Reaction 3.



The zeolite was introduced after the  $\text{Ca}(\text{NO}_3)_2$  had been added to the deionized water resulting in the removal of calcium ions from the solution as shown in Reaction 4.



Since  $\text{Na}^+$  cannot replace  $\text{Ca}^{2+}$  in this chemical reaction, the addition of  $\text{Na}_2\text{CO}_3$  is believed to have no effect on the reacting solution. The formation of calcium carbonate is consequently suppressed resulting in a drop in the pH value of the solution.

### 3. Results and discussion

#### 3.1 X-ray fluorescence (XRF)

The composition of the kaolin and the resulting zeolite samples are presented in Table 1. Silica and Alumina represent the major compounds in the kaolinite, 51.38 and 42.05 wt.% respectively. The amount of  $\text{Fe}_2\text{O}_3$  in the Darazo kaolin is 1.39 wt.% a typical indicator for zeolite synthesis due to the high amount of iron III oxide required to affect the color of the resulting zeolite. Since the calcined kaolin samples both show similar XRF results, only the chemical analysis from the Darazo kaolin calcined at 900°C is given. The XRF of the LTA zeolite shows a significant increase in the the weight percent of the  $\text{Na}_2\text{O}$  (3.42%) present resulting from the addition of NaOH. Other oxides in the Darazo kaolin could not be removed during the zeolite synthesis process meaning that the kaolinite structure is stable even at temperatures of up to 900°C.

**Table 1** Composition of the Darazo kaolinite and the resulting LTA zeolite.

Sample	Composition (weight percent)									
	$\text{SiO}_2$	$\text{Al}_2\text{O}_3$	$\text{Fe}_2\text{O}_3$	$\text{CaO}$	$\text{MgO}$	$\text{Na}_2\text{O}$	$\text{MnO}$	$\text{TiO}_2$	$\text{K}_2\text{O}$	L.O.I
Kaolinite	51.38	42.05	1.39	0.16	0.21	1.73	0.007	2.37	0.43	0.27
Zeolite	68.90	22.76	0.15	0.05	0.05	3.42	0.005	0.01	0.89	3.75

#### 3.2 Fourier Transform Infrared spectroscopy (FTIR)

Figure 1 shows the FTIR spectra of the LTA zeolite produced using Darazo kaolinite. Previously reported kaolinite and metakaolinite spectra were used as a reference [11]. A look at the zeolite spectrum indicates a sharp peak at a wavenumber around  $1000\text{ cm}^{-1}$  which is an exclusive feature of all zeolites that contain the hydrated triple crankshaft chains. This vibration is attributed to a stretching of the T-O bond (T represent a Si or Al ion) which primarily involves motions that are associated with oxygen atoms or alternatively, this can be described as a stretching in the asymmetric mode.

Several differences are observed in the FTIR spectrum of both zeolites, and this can be traced to the degree of crystallinity attained in the samples using different processing temperatures. The symmetric stretching vibration of the  $\text{SiO}_4$  groups can be seen at the transmission peaks between  $700\text{-}750\text{ cm}^{-1}$  which correspond to the presence of internal  $\text{Si-O}\cdots\text{HO-Si}$  bonds. The sharp peaks at a wavenumber of  $1500\text{-}1700\text{ cm}^{-1}$  result from the bending vibrations of  $\text{H}_2\text{O}$  [12]. Various authors assign the peak at  $3300\text{ cm}^{-1}$  to the presence of the OH groups associated with extra framework alumina species and the band at  $3500\text{ cm}^{-1}$  to another type of Al-OH species.

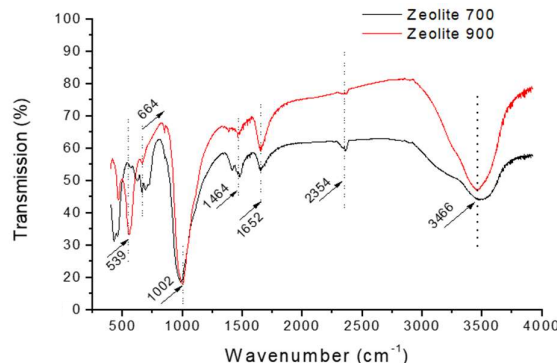


**Figure 1** Fourier transform infrared (FTIR) of the LTA zeolite.

### 3.3 X-ray diffraction (XRD)

High-resolution synchrotron XRD patterns measured at room temperature for the synthesized LTA zeolite is presented in Figure 2. Both zeolites produce similar XRD patterns with the only differences being the peak intensities. This difference shows that the synthesized LTA zeolite prepared by calcining the kaolinite at 900°C has an increase in crystallinity when compared to the kaolinite calcinated at 700°C. The peaks are also similar to those reported for LTA zeolite in the International Centre for Diffraction Data (ICDD) database, 74-1183-ICDD, 2001 [13,14] as well as the work published by the Structural Commission of the International Zeolite Association [15].

The other oxides such as  $\text{Fe}_2\text{O}_3$ ,  $\text{CaO}$ ,  $\text{NaO}$ , associated with the Darazo kaolinite are represented as responsible for the additional peaks in the XRD patterns. The patterns for Darazo kaolin and metakaolin have also been discussed previously [11].

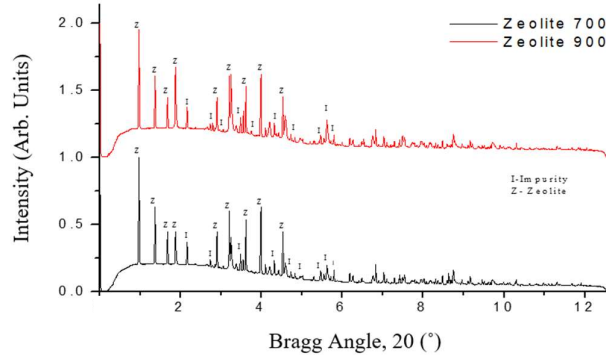


**Figure 2** XRD patterns of the synthesized LTA Zeolites.

### 3.4 Thermal analysis

The TG/DTA results from the synthesized zeolite samples are shown in Figure 3. Very similar trends were observed for both of the LTA zeolite samples. The TG measurement below 350°C resulted in a mass loss of 20.10 and 22 wt.% with an estimated efficiency of 79 and 80% for the zeolite calcined at 700 and 900°C respectively. The initial mass loss from room temperature to about 200°C is associated with the loss of water present in the zeolite.

The mass percentage loss recorded from 200 to 800°C is about 3.75 wt.% and corresponds to the LOI value obtained from the composition analysis represented in Table 1. The data obtained from the DTA show that exothermic reactions are observed for both zeolite samples, but the zeolite calcined at 900°C showed a higher enthalpy of the reaction. A very strong endothermic peak was observed at temperatures of 164 and 175°C for the 700 and 900°C calcined samples respectively and is associated with the loss of chemically combined water. Very little recovery is observed at 265°C and an endothermic transition at 380°C. This may be due to the loss of the lower melting point components in the zeolite.

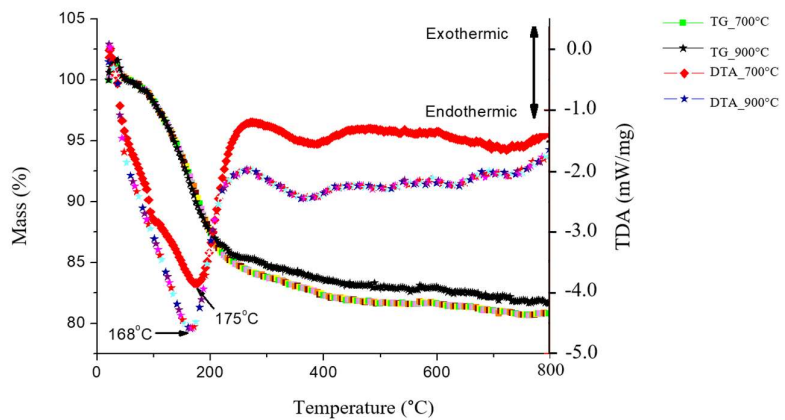


**Figure 3** TG/DTA curves of LTA zeolite samples.

### 3.5. Scanning electron microscopy

The metakaolin and zeolite SEM images are represented in Figure 4. The morphology of the metakaolin is plate-like and appears to be amorphous based as indicated from the XRD pattern. Metakaolin is an amorphous material and has no clearly defined morphology, this is attributed to the highly amorphous nature of the metakaolinite material [16,17]. Crystals with a well-defined cubic structure were observed on the micrograph of the LTA zeolite samples. It can also be seen that aggregates from the gel with the synthesized zeolite are present from the Darazo kaolinite sample prepared by calcining at 900°C. Fewer aggregates were observed from the sample synthesized at 700°C. Large crystals are formed by kaolin and other naturally occurring raw minerals due to the presence of other impurity compounds [18]. These other compounds act as nucleation sites for the formation of the zeolite crystals and result in faster kinetics of crystallization. The type of crystals formed during zeolite synthesis is also influenced by the nature of the metakaolinite used.

Sodalite is usually formed in place of LTA zeolite when kaolin that did not complete the metakaolinization process is used [16]. The shape of the crystals are also affected by the Si/Al ratio for example, when a ratio of 1:5 Si:Al is used, crystals with beveled edges instead of very well defined edges are obtained [19].

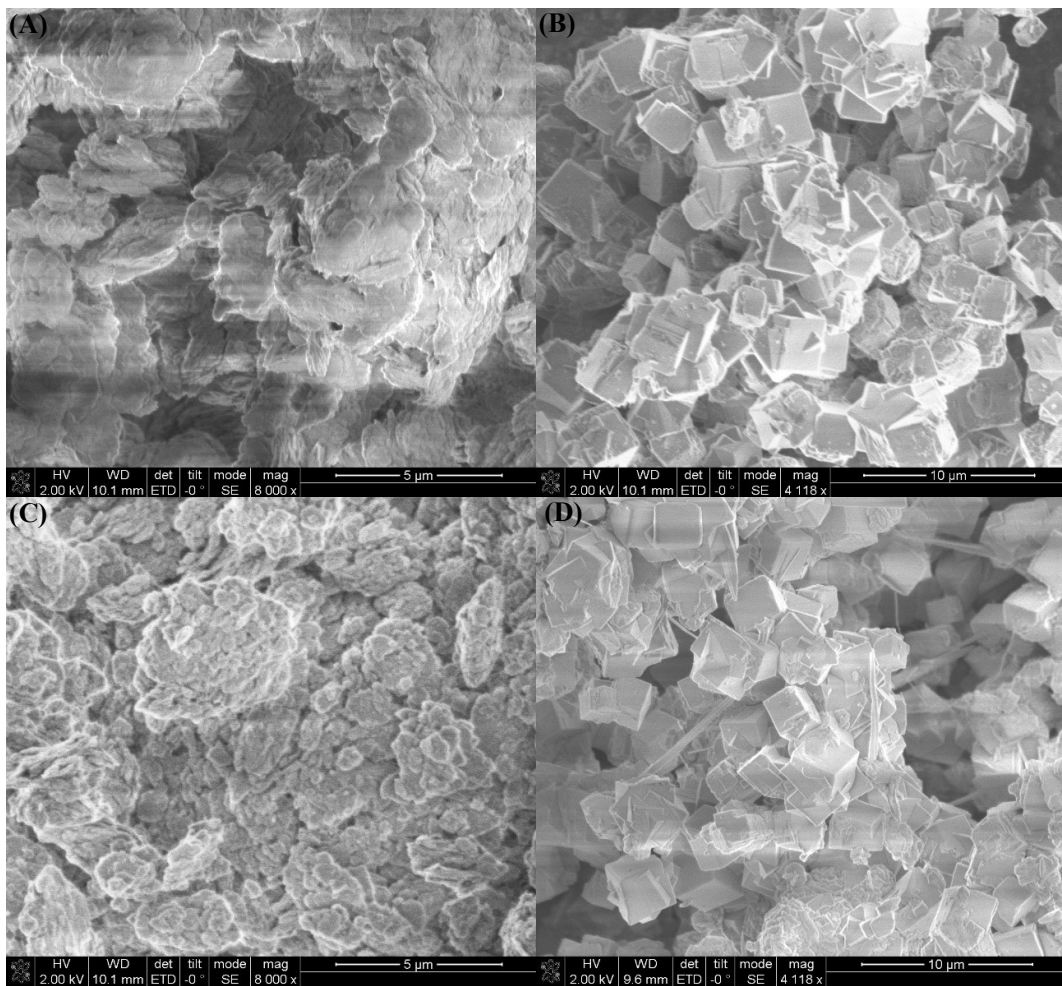


**Figure 4** The SEM for Darazo metakaolin calcined at (A) 700°C and (C) 900°C and LTA Zeolite synthesized from Darazo kaolin calcined at (B) 700°C and (D) 900°C.

### 3.6 BET

The BET and Langmuir surface area, pore size and pore volume of the zeolites are shown in Table 2. Both samples have very low surface areas due to the formation of large crystals which is also correlated with the results seen in the SEM images. This is a result of heterogeneous nucleation since kaolin, the precursor material, contains

minute amounts of other compounds such as CaO, MgO and MnO. Each sample has a reduced surface area as the calcination temperature increases and it is believed that there is a reduction in surface area at higher calcination temperature as a result of the shrinkage and crumbling in the structure of the metakaolinite.

An increase in the calcination temperature produces an increase in the pore volume and pore size as the zeolite produced from kaolin calcined at 900°C has a looser amorphous structure compared to that at 700°C. The pore size of the synthesized LTA zeolite is bigger than those reported for other LTA zeolite synthesized from pure chemicals which is approximately 4 Angstroms [20,21]. The difference in size is possibly due to the difference in the starting raw materials. The use of commercial Al<sub>2</sub>O<sub>3</sub> and SiO<sub>2</sub> as starting materials will lead to fewer impurities when compared to natural kaolin, thus leading to increased heterogeneous nucleation.

**Table 2** BET analysis of the LTA zeolite.

BET Analysis	Zeolite @700°C	Zeolite @ 900°C
Surface area (BET)(m <sup>2</sup> /g)	4.9893	4.6806
Surface Area (Langmuir) (m <sup>2</sup> /g)	5.8277	5.4201
Pore volume (cm <sup>3</sup> /g)	0.007157	0.007534
Pore size (nm)	5.73804	6.43845

Figure 5 shows the nitrogen adsorption/desorption isotherm of the synthesized LTA zeolites. A type IV hysteresis loop is observed as a result of both zeolites being mesoporous. The difference in the curves arises from the difference in calcination temperatures therefore giving the higher temperature zeolite (900°C) a slight tilt which is not present in the 700°C treated sample.

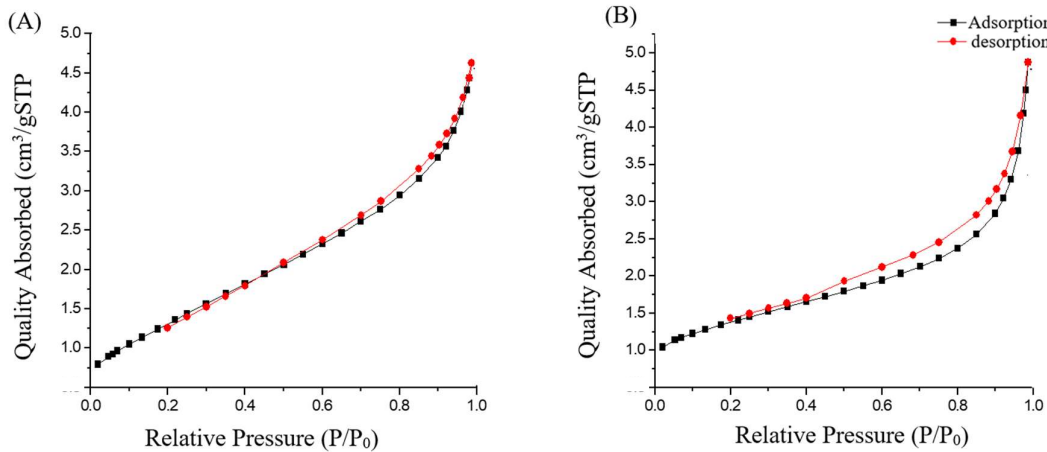


**Figure 5** Nitrogen adsorption/desorption isotherm for the synthesized LTA zeolite (A) 700°C (B) 900°C.

### 3.7. Water adsorption test

The water adsorption capacity data for the synthesized LTA zeolites are shown in Table 3). The water adsorption capacity for the zeolites were found to be 27.96 and 28.01% for samples calcined at 700 and 900°C respectively. The difference in water adsorption capacity is a result of the difference in surface area and the shrinkage of the kaolinite structure. This indicates that the prospects for using this material for water adsorption purposes are highly advantageous since the obtained values are higher than those that are reported for commercial LTA zeolites (25.9 %). This difference is due to the presence of oxides other than the silica and alumina in the kaolin compared to pure silica and alumina [22].

**Table 3** Water adsorption values of the LTA Zeolites.

Water adsorption test	@700°C	@900°C
Beakers Wt. (g)	48.00	83.60
Wt. of Dry LTA Zeolite + Wt. of Beaker (g)	51.07	87.61
Wt. of wet LTA Zeolite + Wt. of Beaker (g)	51.93	88.73
% Water Adsorption	28.01	27.96

#### 4. Conclusion

LTA zeolites with high crystallinity and microporosity were successfully synthesized at calcination temperatures of 700 and 900°C from kaolin found in Darazo region. The LTA zeolite gives promising signs that it can be used as a water adsorption agent, with the 900°C synthesized LTA zeolite giving a better water adsorption capacity. At temperatures below 900°C both zeolites are stable, and the presence of characteristic zeolite peaks confirms the formation of these distinct LTA zeolite crystals. The formation of a cubic structure also confirms an LTA zeolite was produced when calcined at 900°C and has characteristics such as a reduced amorphous gel as well as a metakaolin structure that is well layered. The ion exchange test shows that the synthesized LTA zeolite from Darazo kaolin raw material would serve as a good ion exchange material for future applications.

#### 5. References

- [1] Breck DW. *Zeolite molecular sieve: structure, chemistry and use.* 1<sup>st</sup> ed. New York: WILEY; 1974.
- [2] Chiang AS, Chao KJ. Membranes and films of zeolite and zeolite like materials. *J Phys Chem Solids.* 2001;2(4):145-154.
- [3] Xu R, Yu J, Huo Q, Chen J. *Chemistry of zeolite and related porous materials: synthesis and structure.* 1<sup>st</sup> ed. New York: WILEY; 2007.
- [4] Berendsen W, Radmer P, Reuss M. Pervaporative separation of ethanol from an alcohol-ester quaternary mixture. *J Membr Sci.* 2006;4(8):1-11.
- [5] Chandrasekhar S, Pramada P. Investigation on the synthesis of zeolite NaX from Kerala kaolin. *J Porous Mater.* 1999;2(6):283-296.
- [6] Barrer RM. *Hydrothermal chemistry of zeolite.* 1<sup>st</sup> ed. London: Academic Press; 1982. p. 25-34.
- [7] Atta AY, Ajayi OA, Adefila SS. Synthesis of faujasite zeolites from Kankara kaolin clay. *J Appl Sci Res.* 2007;3(16):1017-1023.
- [8] Yaping Z, Xiaoqiang Q, Weilan Y, Mingwen W. Synthesis of pure zeolite from supersaturated silicon and aluminium alkali extract from coal ash. *Fuel Process Technol.* 2008;8(7):1880-1889.
- [9] Chandrasekhar S. Influence of metakaolinization temperature on the formation of zeolite 4A from kaolin. *Clay Miner.* 1996;31(4):89-95.
- [10] Vaculikova L, Plevova E, Vallova S, Koutnik I. Characterization and differentiation of kaolinites from selected Czech deposits using infrared spectroscopy and differential thermal analysis. *Acta Geodyn Geomater.* 2011;8(6):59-68.
- [11] Kovo AS. Development of zeolites and zeolite membranes from Ahoko Nigerian kaolin [dissertation]. Manchester: University of Manchester; 2011.
- [12] Mgbemere HE, Lawal GI, Ekpe IC, Chaudhary AL. Synthesis of zeolite-a using kaolin samples from Darazo, Bauchi State and Ajebo, Ogun State in Nigeria. *Niger J Technol.* 2018;37(2):87-95.
- [13] Ugal JR, Hassan KH, Ali IH. Preparation of type 4A zeolite from Iraqi kaolin: characterization and properties measurement. *J Assoc Arab Univ Basic Appl Sci.* 2010;9(2):2-11.
- [14] Baerlocher CE, McCusker LB, Olson DH. *Atlas of zeolite framework types.* Amsterdam: Elsevier; 2007.
- [15] Treacy MM, Higgins JB. Collection of simulated XRD powder patterns for zeolites. 5<sup>th</sup> ed. Amsterdam: Elsevier; 2007.
- [16] Reyes C, Williams O, Mauricio R, Alarcon C. Synthesis of zeolite LTA from thermally treated kaolinite. *Rev Fac De Ing.* 2010;53(4):30-41.
- [17] Zhao Y, Zhang B, Zhang X, Wang J, Liu J, Chen R. Preparation of highly ordered cubic NaA zeolite from halloysite mineral for adsorption of ammonium ions. *J Hazard Mater.* 2010;17(6):658-663.
- [18] Petkowicz DI, Rigo RT, Radtke CT, Pergher SB, Santos JH. Synthesis of zeolite NaA from Brazilian chrysotile and rice-husk. *Microporous Mesoporous Mater.* 2008;1(5):548-255.
- [19] Ismail AA, Mohamed RM, Ibrahim IA, Kini GB, Koopman DB. Synthesis, optimization and characterization of zeolite and its ion exchange properties. *Colloids Surf A Physicochem Eng Asp.* 2010;3(6):80-92.
- [20] Farag I, Zhang J. Simulation of synthetic Zeolites-4A and 5A, Manufacturing for green processing, IRACST. *Eng Sci Technol an Int J.* 2012;2(8):188-192.
- [21] Mgbemere EH, Ekpe CI, Lawal IG. Zeolite Synthesis, Characterization and application areas: a review. *Int J Environ Res.* 2017;6(4):45-54.
- [22] Miao Q, Zhou Z, Yang J, Lu S, Wang J. Synthesis of NaA zeolite from kaolin source. *Front Chem Sci Eng.* 2009;3(6):8-17.